2018 Conference on Systems Engineering Research

Exergy Efficiency of Interplanetary Transfer Vehicles

Sean T. Owen[a], Michael D. Watson[b]*, Mitchell A. Rodriguez[c]

[a]*University of Alabama in Huntsville, Huntsville, AL 35899, USA*
[b]*NASA Marshall Space Flight Center, Huntsville, AL 35812*
[c]*Jacobs Space Exploration Group, Huntsville, AL 35806, USA*

Abstract

In order to optimize systems, systems engineers require some sort of measure with which to compare vastly different system components. One such measure is system exergy, or the usable system work. Exergy balance analysis models provide a comparison of different system configurations, allowing systems engineers to compare different systems configuration options. This paper presents the exergy efficiency of several Mars transportation system configurations, using data on the interplanetary trajectory, engine performance, and vehicle mass. The importance of the starting and final parking orbits is addressed in the analysis, as well as intermediate hyperbolic escape and entry orbits within Earth and Marsô s
analyzed include low-enriched uranium (LEU) nuclear thermal propulsion (NTP), high-enriched uranium (HEU) NTP, LEU methane (CH4) NTP, and liquid oxygen (LOX)/liquid hydrogen (LH2) chemical propulsion.

Keywords: Interplanetary; Propulsion System; Sphere of Influence; Systems Engineering; System Exergy; Trajectory

---

* Corresponding author. Tel.: 256-544-3186
E-mail address: Michael.d.watson@nasa.gov

Several space agencies, including NASA, are planning manned exploration of Mars in the upcoming decades. Many different mission architectures have been proposed for accomplishing this. It is the role of systems engineers to compare and optimize different space transportation systems and components, up to and including full mission architectures. To do this, some measure is needed that applies to all systems being compared, even though those systems may have considerable differences. Exergy efficiency, or how well a given system can use the work available to it, provides a measure to compare different interplanetary transfer systems.

Nomenclature

a	=	semimajor axis
F	=	thrust
f	=	final index
G	=	universal gravitational constant
Ωֽ̈	=	s t a n d a r d a c c e l e r a t i o n d u e t o g r a v i t y a t
h_{prop}	=	enthalpy of the propellant
I_{sp}	=	specific impulse
i	=	initial index
KE	=	kinetic energy
m	=	mass
M_E	=	mass of the Earth
M_{planet}	=	mass of the planet
M_{sun}	=	mass of the sun
ά ֽ	=	initial mass
ά	=	mass flow rate
Mvehicle,initial	=	mass of the vehicle on the pad
Mvehicle, final	=	injected mass
PE	=	potential energy
r	=	distance, position, radius
S	=	positive/negative sign
t	=	time
T_{engine}	=	engine thrust
V	=	velocity
ώ	=	acceleration
V_e	=	exhaust velocity
X	=	system exergy
X_{des}	=	exergy destroyed
X_{exp}	=	exergy expended
ɗxg	=	exergy efficiency
ɗ	=	true anomaly
μ	=	gravitational parameter
ű	=	horizon-relative flight angle

1. Exergy Balance Relationship

Planetary transfer vehicles (i.e., satellites, planetary landers, and human and cargo transports as illustrated in Fig. 1) are integrated by system exergy. This includes their propulsion stages, electrical power systems (e.g., nuclear electric or solar electric), and crew volumes for transporting the crew. During propulsive trajectory changes, the exergy balance equation can be written for a spacecraft system as,

[illegible] (1)

The propulsion engine (e.g., chemical, electric, nuclear thermal) characteristics (mass flow, enthalpy, exhaust velocity, and electrical power for electric propulsion) are all included on the left of the equation.

For coast phases of the flight trajectory, the exergy balance equation simplifies to the basic orbital mechanic relationship for a balanced system. In this case the spacecraft energy (and exergy) is constant and the kinetic and potential energies increase and decrease in opposite directions.

[illegible] (2)

This creates an oscillatory relationship between the vehicle kinetic and potential energies with respect to the dominate body (typically the sun in interplanetary space).[i]

Fig. 1. Mars Transfer Vehicle

Planetary and solar masses have a large effect on spacecraft exergy in interplanetary space. It is important to ensure an appropriate reference is used. A heliocentric reference is generally best for space travel within the solar system. When operating within a planetary bodyôs gravitational sphere of influence is greater than the sunôs influence, then centric (geospatial reference system for the Earth) can be used. Equation (3), gives the general relationship for the planetary SOI.[ii]

[illegible] (3)

Planetary transfer uses a Hohmann transfer from Earth to Mars and a Hohmann transfer back to Earth. The planetary stay is also important in calculating the possible trajectories. An 11-month stay on the planet is assumed with a total mission length on the order of two to three years. This trajectory contains four main burns: trans-Mars injection (TMI), Mars orbit insertion (MOI), trans-Earth injection (TEI), and Earth orbit insertion (EOI). Four different propulsion systems were analyzed using this basic course: Low enriched uranium (LEU) liquid hydrogen (LH2) nuclear thermal propulsion (NTP), high enriched uranium (HEU) LH2 NTP, LEU CH4 (methane) NTP, and a chemical liquid oxygen (LO2)/LH2 system.

For the LEU CH4 NTP and CHM LOX-LH2 cases, the mass flow rate for the main engine can be calculated from Ὶ by using Equation (4).

ά ᶻ ᶤ ᶫ ᶻ ᶤ ᶻ ᶻ ᶤ Ὣ ᶤ ᶤ ᶤ ᶤ Ὢ Ὶ Ὶ (4)

The mass flow rate of the reaction control system (RCS) thrusters is an important parameter in the maneuvers for the trajectory burns. For the calculations in this section, the RCS mass flow rate is 7 kg/s with an Ὶ of 291 s.

Fig. 2 shows the exergy efficiency of the LEU LH2 NTP case during the first 500 seconds of TMI, and shows the decline in the efficiency during the RCS burn. Also visible in this plot is an efficiency drop just after the RCS burn; this corresponds to dropping an empty propellant tank. Exergy that was expended to accelerate the tank is lost when the tank is discarded, so dropping the tank registers as a decrease in efficiency.

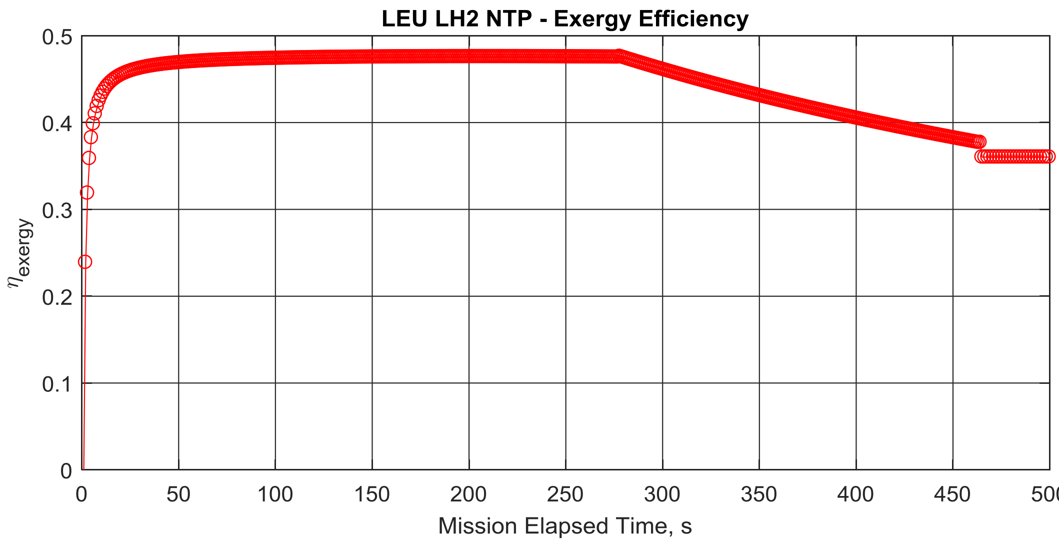

Fig. 2. Exergy efficiency during TMI

Exergy calculations are sensitive to changes in position and velocity with respect to the departure and arrival planets, requiring a complete orbital trajectory to calculate exergy efficiency. A patched-conics trajectory is necessary to show the complete system and planetary environments within each planets SOI and in interplanetary space outside the planets SOIôs.

2. Orbital Mechanics

For each leg of the mission, the departure planet periods when the spacecraft is within the planets SOI.[iii] Outside the planetary SOIôs,

gravity source. Acceleration due to the sun's grav
trajectory path. Fig. 3 shows the spacecraft trajectory path and planets orbital paths during the mission.

Using the planetary positions and the given position of the spacecraft at all points during the mission, the spacecraft's planet-relative distance, speed, and flight angle from the horizon are calculated for the days following the departure burns and leading up to the arrival burns using Equations (5) – (7).

$$\vec{r}_{s/c,rel} = \vec{r}_{s/c} - \vec{r}_{planet} \tag{5}$$

$$\vec{v}_{s/c,rel} = \vec{v}_{s/c} - \vec{v}_{planet} \tag{6}$$

$$\gamma_{s/c,rel} = \cos^{-1}\left(\frac{\vec{r}_{s/c,rel} \cdot \vec{v}_{s/c,rel}}{|\vec{r}_{s/c,rel}|\,|\vec{v}_{s/c,rel}|}\right) \tag{7}$$

Using the spacecraft's planet-relative distance and time, the exact time when it crosses the SOI boundary is interpolated with Equation (8). The two points in time used for the interpolation are those just before and after crossing the SOI boundary, the radius of r_{SOI} defined in Equation (3).

$$t_{SOI} = t_1 + (t_2 - t_1)\frac{r_{SOI} - r_1}{r_2 - r_1} \tag{8}$$

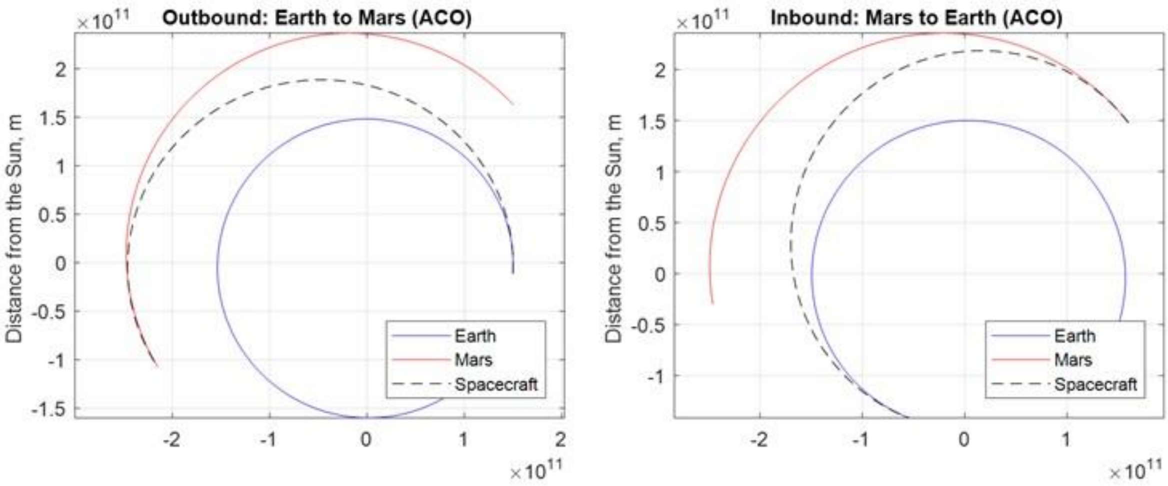

Fig. 3. Spacecraft interplanetary trajectory, and planet trajectories during the outbound and inbound (return) phases

With these values, the planet-relative velocity and flight angle from the horizon at that moment are similarly interpolated using Equations (9) and (10).

$$v_{s/c,rel,SOI} = v_{s/c,rel,1} + (t_{SOI} - t_1)\frac{v_2 - v_1}{t_2 - t_1} \tag{9}$$

$$\gamma_{s/c,rel,SOI} = \gamma_{s/c,rel,1} + (t_{SOI} - t_1)\frac{\gamma_2 - \gamma_1}{t_2 - t_1} \tag{10}$$

Additionally, a new reference frame is created based on the spacecraftôs po
SOI boundary, using Equations (11) ï(13). Planet-centric orbits within the SOI will be plotted in a 2D plane, and this reference frame will track the orientation of the plane relative to the solar ecliptic.

[illegible] (11)

[illegible] (12)

[illegible] (13)

A transformation matrix is created using the new reference frame2 and Equation (14), and will later be used to convert the SOI orbit back to a heliocentric reference frame.

[illegible] (14)

With conditions at the SOI intersection established, the planet-centric transfer and parking orbits within the SOI can be determined. First, the orbitôs semi-major axis is calculated using Equations (15) and (16).

[illegible] (15)

[illegible] (16)

The speed and flight angle of the spacecraft at the edge of the SOI is sufficient to define a hyperbolic orbit past the planet. The parking orbit periapsis is established (400 km ab
orbits at over Earth in this example). This is the
the atmosphere to avoid significant drag. Note, that aerobraking (not addressed here) requires an orbital altitude within the upper atmosphere with sufficient drag to reduce the spacecraft velocity (DV) to enter the prescribed parking orbit. Equations (17) ï(4.66) are used to determine the apoapsis of the parking orbi

[illegible] (17)

[illegible] (18)

[illegible] (19)

[illegible] (20)

[illegible] (21)

[illegible] (22)

It is important for the apoapsis to remain within … meet the parking orbit period necessary to meet mission objectives. Once the apoapsis and periapsis are established, the parking orbit periapsis is kept as the periapsis of the hyperbolic transfer orbit. This results in an extremely elliptical parking orbit with a very long period (particularly if it extends to the planetary SOI boundary). Equations (4.61) – (4.66) can be solved iteratively starting with an initial periapsis estimate and stepping in small increments (e.g., 100 mi periapsis altitude increases) until a reasonable apoapsis is found.

The eccentricity of the hyperbolic transfer orbit, … velocity can be calculated using Equations (17), (18), and (23).

$$[illegible] \tag{23}$$

By applying the listed … point-thrust burn, the shape of the new parking orbit around the planet can be approximated using Equations (19) – (21). It is only an approximation because it assumes a point-thrust burn connects the transfer and parking orbit. As long as the chosen propulsion system is sufficiently high-thrust, the actual parking orbits will be quite close to the listed values here, as a sufficiently short burn time (on a timescale of minutes) will be negligible compared to the period of the parking orbit.

The parking orbits are only an approximation based on point-thrust burns. In order to properly calculate the exergy efficiency, plots of the spacecraft's position and … To do this, Equations (24) and (25) can be used to track the spacecraft forwards or backwards in time from periapsis to establish its trajectory. Another acceleration vector from the spacecraft's engine is added, aimed d… point in time for backward tracking. This new vecto…

$$[illegible] \tag{24}$$

$$[illegible] \tag{25}$$

At this point, a complete planet-centric course contains the spacecraf… SOI exit (or vice versa for entry scenarios). This course is then rotated such that the SOI exit/entry point lies di… on the i… -centric reference frame. Equations (26) and (27) are then used to … heliocentric position and velocity while it is inside the SOI.

$$[illegible] \tag{26}$$

$$[illegible] \tag{27}$$

3. Interplanetary Exergy Efficiency

With the modified mass data and orbital data in hand, the actual exergy calculations can begin. During each burn of the mission, changes in expended exergy are calculated using Equation (28) which is taken from Equation (1), with mass drops for each time step being calculated from the tank drops and consumable use schedules. These step changes are then summed to produce a plot of expended exergy that rises during burns but otherwise stays constant.

$$[illegible] \tag{28}$$

In order to calculate destroyed exergy, changes in kinetic and potential energy must be tracked across the entire mission. To determine whether the change in kinetic or potential energy should be positive or negative during a given time step, the ruleset described below in Table 1 is applied, based on Equations (29) and (30). Changes in the spacecraftôs velocity and distance relative to the determining the sign. It should be noted that the values X, Y, and Z in the table are all greater than or equal to one.

Table 1. Sign convention for changes in kinetic and potential energy

Mass	Velocity	ΔKE_{step}	Distance	ΔPE_{step}
[illegible]	[illegible]		[illegible]	
[illegible]	[illegible]		[illegible]	
[illegible]	[illegible]		[illegible]	[illegible]
[illegible]	[illegible]		[illegible]	[illegible]
[illegible]	[illegible]	[illegible]	[illegible]	
[illegible]	[illegible]	[illegible]	[illegible]	
[illegible]	[illegible]	[illegible]	[illegible]	
[illegible]	[illegible]	[illegible]	[illegible]	
[illegible]	[illegible]		[illegible]	[illegible]
[illegible]	[illegible]		[illegible]	[illegible]

[illegible] (29)

[illegible] (30)

Change in kinetic and potential energy during a given time step is then calculated using Equations (31) and (32), where S is the sign taken from the previous table, either 1 or -1.

[illegible] (31)

[illegible] (32)

These step changes in kinetic and potential energy are summed over time to create a running total of energy changes. These sums are subtracted from the expended exergy using Equation (33) to calculate the exergy destroyed, which then directly leads to the exergy efficiency, defined in Equation (34), at that point in time.

[illegible] (33)

[illegible] (34)

When the spacecraft is within a planetôs SOI and fluctuates with the planetary gravity influences as the vehicle and planet both move along their respective trajectories. This is avoided by using a patched-conics model for the orbital modifications, where exergy calculations are applied

to each SOI independently, not using the heliocentric portion of the trajectory. Whenever the spacecraft crosses into or out of a SOI, the most recent value for the total change in kinetic and potential energy is carried over to the next series of calculations. This ensures that exergy ef
are constant, even across SOIs.

The final exergy efficiency plots over the whole mission for each propulsion system are given below in Fig. 4 through 7.

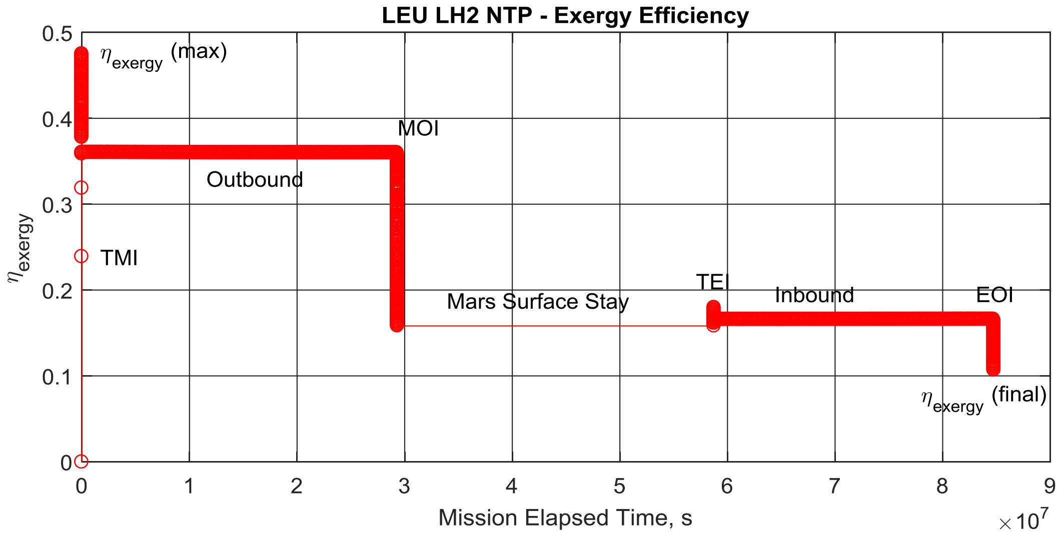

Fig. 4. Exergy efficiency throughout the mission using the LEU LH2 NTP system.

As seen previously in Fig. 2, exergy efficiency will sharply rise when using a main engine during a departure burn, and then decrease during the following RCS burn. Th $_{sp}$ destroying more exergy for the same exergy expenditure, thus lowering the efficiency of that stage of the mission. Efficiency also drops when ejecting an empty propellant tank or spent consumables, as the exergy expended to move those components up to speed is lost when they are discarded.

References

[i] :DWVRQ 0 ' ³6\VWHP ,QWHJUDO 6\VWHP 3K\VLFV RI /DXQFK 9HKLFOHV
Spacecraft and Rockets, January 2018.

[ii] &XUWLV +RZDUG ' ³2UELWDO 0HFKDQLFV IRU (QJLQHHULQJ 6WX 3rd ed., Elsevier, Boston, 2014.

[iii] NASA-SP-2009-566, Human Exploration of Mars Design Reference Architecture 5.0, Addendum #2, March 2014.